The Maintenance of Low-Frequency Atmospheric Anomalies

GRANT BRANSTATOR

National Center for Atmospheric Research, Boulder, Colorado*

(Manuscript received 18 June 1991, in final form 9 January 1992)

ABSTRACT

A linear budget is used to ascertain which of several proposed processes are most important in maintaining four prominent low-frequency perturbation patterns in a perpetual January general circulation model simulation with fixed ocean temperatures. In the budget technique the time-average model equations are separated into those terms that are in common with the steady, adiabatic linearized form of the model equations and the remaining terms, which are treated as forcing terms. By examining the linear response to each of these forcing terms for prominent episodes of the low-frequency patterns, the terms that are most important in maintaining the low-frequency patterns can be determined.

The results indicate that interactions between the low-frequency patterns and the time-mean zonal asymmetries of the model climate are crucial to the maintenance of the patterns. Of equal importance are anomalous fluxes from transients, without which the low-frequency anomalies would not be maintained. Vorticity fluxes due to bandpass (1–7 days) fluctuations ranging over broad sectors of the globe are found to be the most important components of the maintaining flux anomalies. Of secondary importance are nonlinear interactions of the low-frequency deviations with themselves. For some patterns this interaction acts to skew the distribution of observed amplitudes. It is also found that the influence of the zonal-mean component of low-frequency perturbations on the remaining low-frequency perturbation components can be appreciable.

Charts of the ability of point sources of heat and vorticity to excite the low-frequency patterns are used to interpret the budgets. These plots indicate that, in a system with time-dependent ocean temperatures, diabatic anomalies could be more instrumental in maintaining low-frequency anomalies than they are in the currently studied model. Midlatitude ocean temperature appears to be especially important in this regard. However, the collocation of regions with pronounced low-frequency anomalous vorticity fluxes from high-frequency transients and regions from which the low-frequency patterns are easily stimulated means that even if varying bottom boundary conditions are present, low-frequency maintenance by transients should continue to be important. The point source results also show that the maintaining transients are not configured optimally for forcing the low-frequency patterns. This indicates that some organizing mechanism must be affecting the maintaining transients.

1. Introduction

As has been documented by a plethora of investigations during the past decade, a surprisingly large fraction of the variance in low-frequency wintertime, midlatitude, Northern Hemispheric flow is produced by a handful of geographically fixed circulation patterns. Given the potentially destructive processes at work in the atmosphere—instability, dispersion, nonlinearity, dissipation—it is not clear how these special structures are maintained for long periods of time. This is not to say that explanations are not available. On the contrary many, possibly competing, mechanisms for maintaining these low-frequency anomalies have been suggested by numerous researchers. This paper describes the results of a diagnostic study that has been undertaken to test the relative importance of these various mechanisms.

The maintenance mechanism that we investigate can be divided into five more or less distinct classes. First is the notion that the anomalies are remotely forced by tropical heating anomalies whose influence is transferred to midlatitudes through the dispersive properties of planetary waves. Similarities in the structure of wave trains induced by isolated vorticity sources (as in Hoskins et al. 1977) and flow anomalies associated with tropical Pacific warm events (as in Horel and Wallace 1981) support this concept. Second is the possibility that midlatitude high-frequency transients may act to force low-frequency anomalies. Egger and Schilling (1983) demonstrated the feasibility of this, and recently Metz (1989), Lau (1988), and Nakamura and Wallace (1990) have provided observational evidence of this mechanism. Third is the idea that the low-frequency anomalies may be stationary solutions to the governing equations that rely on steady nonlinearities for their self-maintenance. Structural similarities between

* The National Center for Atmospheric Research is sponsored by the National Science Foundation.

Corresponding author address: Dr. Grant Branstator, NCAR, P.O. Box 3000, Boulder, CO 80307.

spherical modons (e.g., Tribbia 1984; Verkley 1984) and atmospheric blocks, and between the more general free solutions of Branstator and Opsteegh (1989) and certain flows in nature, add credence to this possibility. Fourth is the suggestion that anomalies in quasi-stationary waves may be caused by modifications to the propagation characteristics of the atmosphere that result from changes to the zonal-mean flow. The work of Branstator (1984), Kang (1990), and Nigam and Lindzen (1989) has shown that effect can be important in both nature and general circulation models. Fifth is the concept that zonal variations in the time-mean state can act to qualitatively modify low-frequency anomalies induced by other means (as in Simmons 1982 and Branstator 1983), or can serve as internal sources of energy for the perturbations (as in Simmons et al. 1983; Branstator 1985). Together these effects of the zonal asymmetries can lead to the natural selection of structures that match the low-frequency structures that recur in nature and general circulation models (as in Simmons et al. 1983; Frederiksen 1983; and Branstator 1990).

To distinguish these various mechanisms we perform a linear diagnostic analysis of some prominent low-frequency patterns. This technique, which is more fully described in section 2, allows quasi-stationary perturbations to be interpreted as the linear response of the primitive equations to forcing by anomalous diabatic heating anomalies, anomalous transient eddy fluxes, and nonlinearities that result from self-interaction of the steady perturbations. Since the effects of the various forcing terms are additive, by applying the technique to episodes of the leading patterns, one can determine the effect of each maintenance term separately. This approach has been used by Nigam et al. (1986) and Valdes and Hoskins (1989) to analyze the maintenance of the climatological stationary waves, and by Kok and Opsteegh (1985) and Held et al. (1989) to separate the effect of diabatic and transient terms on forcing flow anomalies associated with ENSO.

A drawback of the linear diagnostic technique is that it requires comprehensive global data of both the climate of the atmosphere and the state of the atmosphere during the episodes of interest. The inaccuracy of current analyses of the divergent circulation, high-frequency transients, and diabatic terms may lead to difficulties in such an analysis, as pointed out by Trenberth and Branstator (1991). We have chosen to avoid this difficulty by analyzing the prominent low-frequency patterns of a general circulation model (GCM). As first pointed out by Lau (1981), GCMs can produce very realistic low-frequency structures, and the fact that essentially complete knowledge of their states is obtainable makes their simulations a good data source for our study. The low-frequency structures whose maintenance we examine are described in section 3.

We begin our analysis, in section 4, by performing a linear budget that uses an operator linearized about the zonal-mean climate from the GCM. Because the primary finding of that calculation is the prominent role played by interactions between the slow perturbations and zonal undulations in the climate state, in section 5 we redo the budget with this interaction incorporated into the linear operator. This analysis strongly suggests that anomalous transient eddy fluxes are the primary means of maintaining the low-frequency anomalies in this GCM. Characteristics of these transients, as well as of the stationary nonlinearities, which act to limit the amplitude of some anomalies, are examined in section 6. Section 7 points out difficulties with the approach used in the investigation. Section 8 discusses the conclusions that can be drawn from the study, shows how some of the results are related to the optimal excitation of the patterns in a linear model, and lists implications the findings have on the possibility of extended-range forecasting.

2. Low-frequency patterns in a GCM

The low-frequency structures that interest us are found in a 6000-day perpetual January simulation produced by Version 0B of the Community Climate Model (CCM) of the National Center for Atmospheric Research. The formulation of this nine-level, rhomboidal-15 model has been described by Williamson (1983), and characteristics of its climate are outlined by Williamson and Williamson (1984).

As noted by Branstator (1990), the vertical structure of low-frequency variability in this model is largely equivalent barotropic with maximum variance in the velocity fields in the upper troposphere. Thus, we use streamfunction at the $\sigma = 0.336$ level (denoted $\psi_{0.336}$) to identify prominent low-frequency patterns in the simulation. This is done by Fourier filtering $\psi_{0.336}$ in time so that only periods longer than 60 days are retained, and then performing an empirical orthogonal function (EOF) analysis of the filtered fields. The EOFs are derived from a covariance matrix based on semi-spectral, latitude-weighted, spatial Fourier coefficients. Such an analysis produces prominent low-frequency patterns of deviations from the 6000-day mean. In this paper when we refer to "anomalies," without qualifications, we mean such deviations.

The leading EOFs are virtually identical to those reported by Branstator (1990) for monthly means from this same simulation. The first three represent 17%, 10%, and 6% of the variance of the filtered data. Our study is concerned with the second and third of these EOFs, which we refer to as EOF2 and EOF3. As shown by Branstator, the leading EOF is primarily a tropical pattern, which has little to do with the low-frequency behavior of the geopotential field, and we will not consider it in this study of midlatitude structures. The leading two EOFs of similarly filtered 300-mb geopotential fields clearly represent the same phenomena as

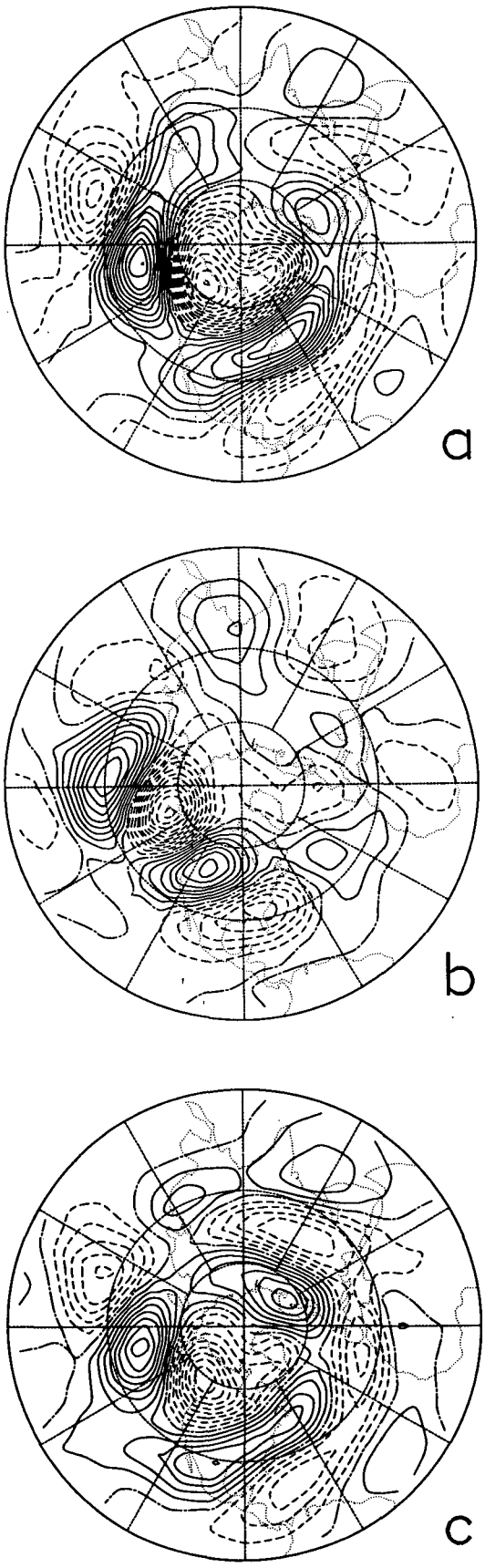

our second and third streamfunction EOFs and explain 19% and 9% of the variance.

To produce fields associated with these EOFs, we employ composites. Throughout this study composites are formed by averaging unfiltered fields from those 600 days during the simulation when temporally filtered $\psi_{0.336}$ projects most strongly onto a particular EOF. To take into account the possibility that patterns with the same structure, but opposite polarity, may behave differently, we average days with projections of a single sign, which means that for each EOF we typically produce two composites. Examples of two such composites are shown in Fig. 1. They are composites of the deviation of $\psi_{0.336}$ from the 6000-day average. Figure 1a shows the composite for positive projections onto the second streamfunction EOF (which we henceforth refer to as EOF2+) and, as one would expect, its structure matches the structure of EOF2. It is a circulation that has most of its variance in the Pacific and North American regions and a distinct zonally symmetric component. The composite of $\psi_{0.336}$ deviations for days with positive projections onto EOF3 is shown in Fig. 1b. It is roughly in spatial quadrature with EOF2, but does not have a prominent zonal-mean component. Composites for projections of the opposite sign have structures that are nearly identical to these two patterns and are not displayed. As described in Branstator (1990) the vertical structure of three-dimensional composites for these patterns is strongly equivalent barotropic. These, then, are the low-frequency patterns whose maintenance we wish to understand.

3. Diagnostic techniques

Derivation of the diagnostic equations that we use to determine how the CCM low-frequency anomalies are maintained can be demonstrated by focusing on a few terms in the thermodynamic energy equation. If the variables in that equation are decomposed into their time-average values from the 6000-day simulation, denoted $\overline{(\ )}^c$, and deviations from that average, denoted $(\ )'^c$[1], then the time-average equation takes the form

$$\overline{T}_t^c + \bar{u}^c \overline{T}_x^c + \overline{u'^c T'^c_x}^c + \cdots - \kappa\nabla^2\bar{T}^c + \overline{D_T}^c = \bar{Q}^c \tag{1}$$

[1] Unless stated otherwise, in this paper the word "transients" refers to the component of the flow denoted by a prime, i.e., departures from a time mean.

FIG. 1. Average $\psi_{0.336}$ anomalies for those 600 days of a 6000-day simulation that have the strongest positive projection onto (a) EOF2 and (b) EOF3, when the EOF analysis is performed on $\psi_{0.336}$ data filtered to retain periods longer than 60 days. (c) Same as (a) except the zonal mean is removed. Contour interval is 1×10^6 m^2 s^{-1}.

where Cartesian coordinates have been used for simplicity, T is temperature, u is the zonal wind component, κ is the CCM horizontal diffusion coefficient, D_T is CCM thermal vertical diffusion (including the effects of surface sensible heat fluxes), and Q stands for the diabatic terms in the CCM (other than sensible heating). A similar time-average equation can be written for a subset of the days in the simulation, for example, those days included in one of our composites. In that equation variables are decomposed into the time average from those days, $\overline{(\ )}^s$, and deviations from that average, $(\ )'^s$. If (1) is subtracted from the time-average equation of the subset and $\hat{(\ )} = \overline{(\ )}^s - \overline{(\ )}^c$ denotes the time-average deviation of the subset from the climate average, our budget equation results

$$\hat{u}\overline{T}_x^{\,c} + \bar{u}^x\hat{T}_x + \cdots - \kappa\nabla^2\hat{T} = -\hat{T}_t - \overset{A}{\hat{u}\hat{T}_x} - (\overset{B}{\overline{u'^sT'^s_x}^s} - \overline{u'^cT'^c_x}^c) - \cdots - \hat{D}_T + \hat{Q}. \quad (2)$$

Companion equations for vorticity, divergence, and surface pressure anomalies can be derived in a similar manner from the other prognostic equations of the CCM.

Terms on the left-hand side of (2) and its companion equations are formally the same as the terms in the multilevel linearized primitive equations. Thus, the time-average deviations can be interpreted as being the steady response of the primitive equations linearized about the climatological state to forcing by the quantities on the right-hand side of (2) and its companions. No approximations have been made in the budget equations. If one calculates each forcing term with the same numerical procedures used in the CCM and uses them to force the linear system, the steady response should be exactly equal to the time-average perturbations. Since the left-hand operator is linear, the effect of the various forcing terms is additive and their individual contribution to the maintenance of the time-average deviations can be determined.

A few modifications to this diagnostic approach must be made before it can be applied to the CCM composites of section 2. The linear operator is of too high an order to be used in a practical manner. This can be overcome by spectrally truncating basic-state and time-average deviation fields on the left-hand side, as well as all terms in the equations, to a manageable level. To keep the linear budget equations exact, this truncation requires the addition of new forcing terms to account for the projection of interactions between unrepresented scales, and between represented and unrepresented scales, onto the represented scales. We truncate the linear model at zonal wavenumber 10 but keep the full complement of 16 meridional modes for each zonal mode, and (as shown in sections 4 and 5) we find this additional forcing is small.

Augmentation of the dissipation in the budget operator is a second modification that must be done to the scheme. As explained in the Appendix, without this dissipation the linear operator is unphysically sensitive to details of the forcing distribution. We use the same horizontal and vertical dissipation employed by Branstator (1990). With this dissipation the operator has the desirable attribute that its near resonances are similar to some of the low-frequency patterns found in the climate integration of the CCM. As described in the Appendix, the linear dissipation is a close enough approximation to the CCM's more complicated dissipation terms that when the viscous linear operator is forced by the right-hand-side terms valid for a particular composite [and the diagnosed anomalous dissipation, like $\hat{D}_T$ in (2), is not included as forcing] the linear response is very similar to the composite. Thus, even though the budget equations are no longer exact, we can continue to interpret the composite anomalies as the linear response to the various forcing terms.

To simplify the budget, we ignore the time-average tendency of anomalies, like $\hat{T}_t$. Because we apply the budget equations to composites based on a daily index crossing a threshold, one would expect the tendency terms to be very small in our calculations, and they are.

A final modification to the budget must be made to overcome the fact that a complete representation of the CCM simulation is not available. Model output is archived every 12 simulated hours so the highest-frequency transients are not accounted for, and the effective thermal source that results from convective adjustment is not archived. We deal with these shortcomings by calculating the effects of the unsampled momentum fluxes as a residual; finding them small, we assume the effects of the unsampled thermal fluxes are negligible. Furthermore, we calculate the convective adjustment heating as a residual. Numerous checks show that no spurious sources are introduced by these calculations of residuals.

The linear budget we have thus far formulated differs from linear budgets mentioned in the Introduction, in that our linearization is about a state that includes zonal variations. The more conventional budget, which employs a zonally symmetric basic state, can be produced by simply decomposing the basic state on the left-hand side of our budget into zonal mean and zonal departures, and moving the resulting terms that include these zonal departures onto the right-hand side. Thus, terms like $-\bar{u}^c{}_*\hat{T}_x$, where $(\ )_*$ is the departure from the zonal average, become forcing terms. Denoting zonal-mean quantities with square brackets, the thermal budget equation with this more conventional basic state is

$$[\bar{u}^x]\hat{T}_x + \cdots - \kappa\nabla^2\hat{T} = -\hat{T}_t - \overset{A}{\hat{u}\hat{T}_x} - (\overset{B}{\overline{u'^sT'^s_x}^s} - \overline{u'^cT'^c_x}^c) - (\overset{C}{\bar{u}^c_*\hat{T}_x + \hat{u}\bar{T}^c_{*x}}) - \cdots - \hat{D}_T + \hat{Q}. \quad (3)$$

Just as with the budget involving an asymmetric basic state, this equation must be modified. The terms represented by $\hat{D}_T$ are replaced by linear dissipation terms incorporated into the left-hand side, and new forcing terms to counteract truncation of fields to zonal wave 10 are included. In addition, the zonal-mean component of each term is removed, so that the budget is concerned with the maintenance of only the zonally asymmetric component of time average anomalies. Equation (3) so modified, together with companion equations for vorticity, divergence, and surface pressure, constitutes the conventional linear budget with which we begin our analysis.

4. Linear budget with a symmetric basic state

The power of the linear budget technique is that one can use it to interpret the impact of individual processes in maintaining a flow anomaly. The particular processes considered depend on the way in which the budget forcing terms are subdivided. For budgets that use the conventional zonally symmetric basic-state operator we have divided the forcing into (i) anomalous latent heat release and convective adjustment, (ii) anomalous radiation [together (i) and (ii) make up $\hat{Q}$ in (3)], (iii) anomalous transient fluxes (term B in equations (2) and (3) being an example of this), (iv) stationary nonlinearities (like term A), (v) anomaly interactions with climatological zonal asymmetries, which we often refer to as the interaction term (term C), (vi) interactions involving unresolved climatological or anomalous flow. By considering the response of the linear model to each of these we can determine how moist processes, radiation, transients, nonlinearities, climatological undulations, and truncated interactions are contributing to the maintenance of the low-frequency CCM anomalies.

One measure of the importance of a process in maintaining an anomaly is the strength of the linear response it excites. The plots in Fig. 2 of the standard deviation of the $\psi_{*0.336}$ response to each of the six forcing types for each of the four EOF composites give this kind of information. Comparison of these to each other and to the strength of the composite, which is also plotted in Fig. 2, shows clearly that some maintenance terms are of little importance. For each composite the response to radiation anomalies is negligible, even though an interactive cloud parameterization is employed in the CCM. The effect of truncation is also small, indicating that truncating the climatological fields and time-average perturbations at zonal wavenumber 10 has little influence on the budget. The response to nonradiative diabatic heating and to stationary nonlinearities is substantial, but not dominant. In all four composites it is the response to anomalous transient fluxes and the effect of the climatological asymmetries through interaction terms like C that make the largest contributions to maintaining the flow

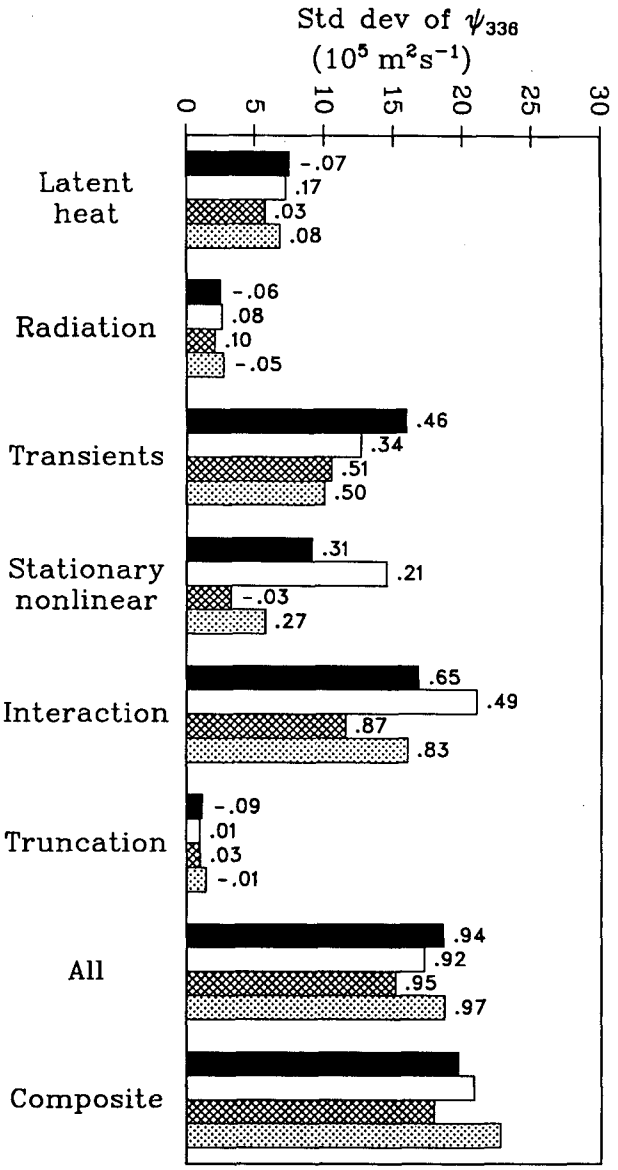

FIG. 2. Spatial standard deviation of $\psi_{*0.336}$ for the response of a model linearized about a zonal-mean basic state to anomalies of latent heating and convective adjustment, radiation, transient fluxes, stationary nonlinearity, climatological wave time-mean anomaly interactions, truncation, and the sum of all these for composites of EOF2 and EOF3. Solid bars are for EOF2+, open bars are for EOF2−, cross-hatched bars are for EOF3+, stippled bars are for EOF3−. Also plotted is the spatial standard deviation of each composite with zonal means removed. Above each bar is the spatial correlation of the linear response and the composite.

anomalies. The values depicted in Fig. 2 indicate that for each composite the sum of the variances of the responses to the various forcing components is considerably stronger than the variance of the response to the sum of the forcing components. This means there is cancellation in the effects of the various processes. (The response to the summed forcing does not exactly

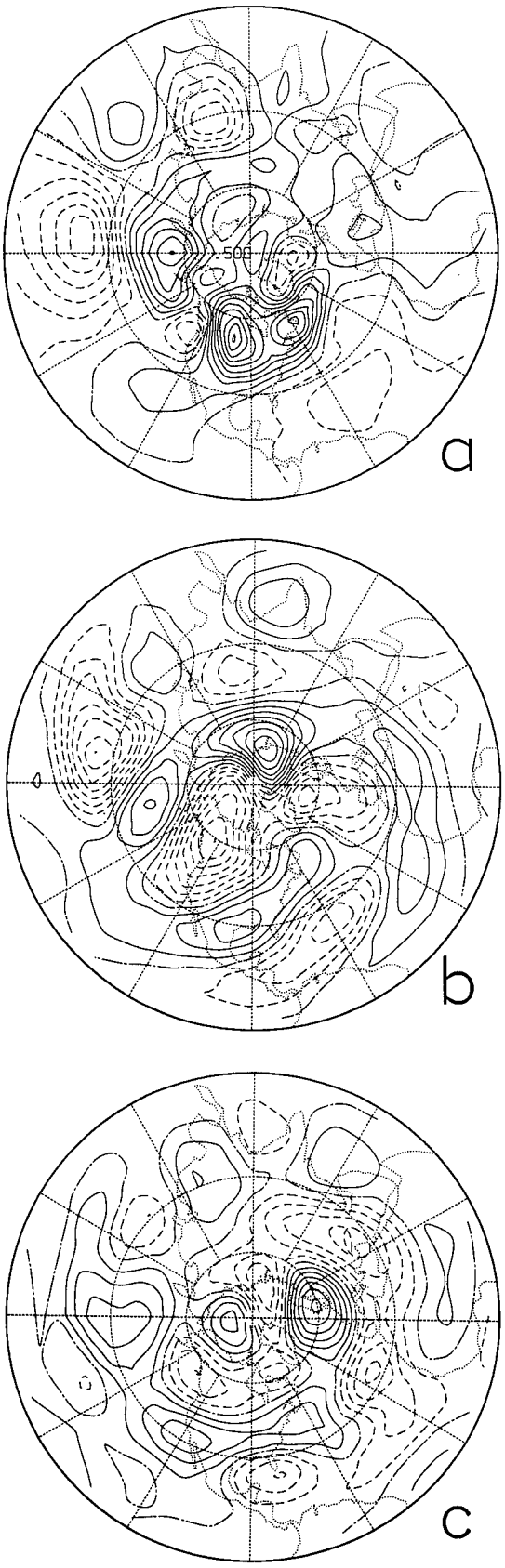

match the strength of the composite because of differences in dissipation in the linear budget and in the CCM.)

Another measure of the contribution made by each type of forcing is the pattern correlation between its linear response and the composite. This measure, which is also plotted in Fig. 2, reinforces the indication given by the standard deviation that anomalous transient fluxes and interactions with the climatological waves make the most important contributions to all of the composite patterns. Though contributions from these influences seem about equal for the two EOF2 composites, by this measure the interaction terms are the dominant effect in producing the two EOF3 composites. This is in keeping with the investigation of Branstator (1990), who found that even with random distributions of steady forcing, EOF3 would be a prominent pattern, provided the effect of the CCM's climatological asymmetries was allowed to operate.

To see how the interaction terms, which are often ignored in a linear budget, are helping to maintain the low-frequency anomalies, we consider the EOF2+ composite. We have found that those components of these terms in the vorticity equation have the strongest effect on the linear solutions. In Fig. 3a is depicted the inverse Laplacian of the vorticity forcing (i.e., the streamfunction forcing) at $\sigma = 0.500$ from the interaction terms before the zonal mean has been removed. The structural similarity between this forcing and the anomalies (Fig. 1a) it helps to maintain is apparent. The location of the strongest forcing in the central northern Pacific and west Atlantic is reminiscent of Simmons et al. (1983) and Branstator's (1985) finding that barotropic eigenmodes that grow via the interaction term gain energy in the jet exits, where zonal gradients in the climatological flow are strong.

The response of the linear model with the zonal-mean basic state to the interaction terms for the EOF2+ composite is displayed in Fig. 3b. The response to the remaining forcing terms in the linear budget is in Fig. 3c; this is the approximation to EOF2+ that most linear budgets, by ignoring the interaction terms, would give. Comparison with a composite of EOF2+ that has the zonal mean removed (Fig. 1c) indicates that the interaction terms are responsible for the arching structure of the pattern. The remaining terms produce features of roughly equal amplitude that tend to amplify or elongate the features produced by the interaction term. Inspection of similar plots for the other composites reinforces the impression that forcing produced by in-

FIG. 3. (a) Forcing of $\psi_{*0.500}$ due to interactions between EOF2+ composite anomalies and zonal asymmetries of the climatological flow. Contour interval is 4 $m^2 s^{-2}$. (b) Linear response of $\psi_{*0.336}$ to the zonally asymmetric component of the forcing displayed in (a). (c) Linear response to all other maintenance terms during the EOF2+ episodes. Contour interval for (b) and (c) is 1×10^6 $m^2 s^{-1}$.

teractions between the climatological flow and the low-frequency anomalies is primarily responsible for maintenance of the low-frequency anomalies.

5. Linear budget with an asymmetric basic state

Having found the key role played by interactions between low-frequency anomalies and the climatological waves in maintaining the low-frequency anomalies, we turn to a linear budget that includes this term in the linear operator, that is, one based on equations like (2). In this way we can see the effect of the other forcing terms when the perturbations they produce are influenced by the important interaction they have with the climatological waves. It should be noted that by moving this interaction to the left-hand side of our budget equations we truly are incorporating an important component of the maintenance processes into the operator. One can imagine a situation in which one adds a large term to the operator but, because it is not physically relevant, a similar large term must be added to the forcing to balance it. This is not the situation when we include the interaction term in our operator. In fact, the total forcing required to maintain each composite is markedly weaker for the linear budget with the asymmetric basic state than it is for the budget with the zonally symmetric state.

With the more complicated operator we subdivide the forcing terms into exactly the same terms used for the preceding analysis, except there is now no explicit forcing due to the interaction between anomalies and basic-state zonal inhomogeneities. The strength of the steady linear response to each of these forcing terms for each composite is given in Fig. 4. For each flow pattern the response to anomalous transient fluxes is by far the strongest, while the influence of latent heating and stationary nonlinearities is nonnegligible. Pattern correlations (Fig. 4) between the linear response to the individual maintenance terms and the composite patterns also indicate that transients are primarily responsible for maintaining the anomalies. (Pattern correlations between composites and the response to the sum of the forcing terms are smaller in this case than for the calculation with a zonally symmetric basic state. This decreased accuracy in the budget is a consequence of the increased volatility of the linear operator that results from incorporating the interaction term into the linear operator, an effect referred to in the Appendix.)

The summarizing statistics of Fig. 4 indicate that, provided the effects of interactions with the climatological flow are accounted for implicitly, the leading low-frequency anomalies in the CCM are primarily maintained by transients. On the other hand, the significant amplitude of the response to diabatic heating and stationary nonlinearities means that regionally these could also be important. To investigate this possibility we examine plots of the linear response to these terms as well as to anomalous transients.

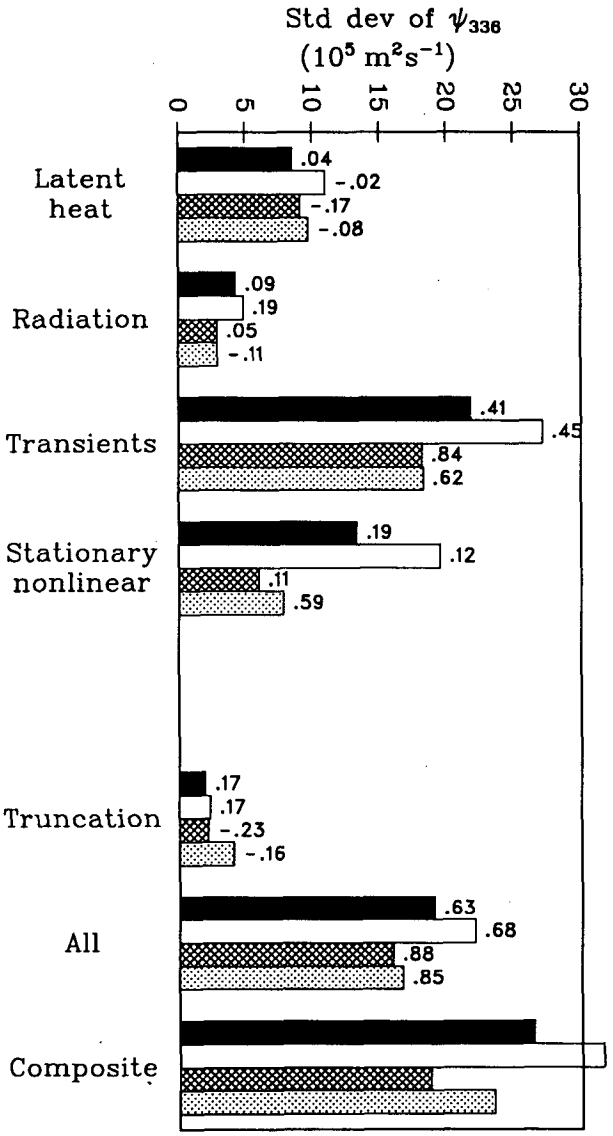

FIG. 4. Same as Fig. 2 except the responses are for a model with a three-dimensionally varying basic state and zonal means are included.

The steady response to the anomalous transient fluxes that occur during episodes of EOF2+ is shown in Fig. 5c. Virtually every feature in the corresponding $\psi_{0.336}$ composite of EOF2+ (Fig. 1a) is in this chart. Even relatively minor circulations over southern Asia are captured. The forcing that produces this response is represented in Fig. 5a by the anomalous transient flux forcing of $\psi_{0.336}$. (We use this field to represent the forcing by transients because, as shown in section 6, of all the transient forcing fields, vorticity forcing at $\sigma = 0.336$ has the largest influence on our composite flows.) In agreement with Lau's (1988) observational

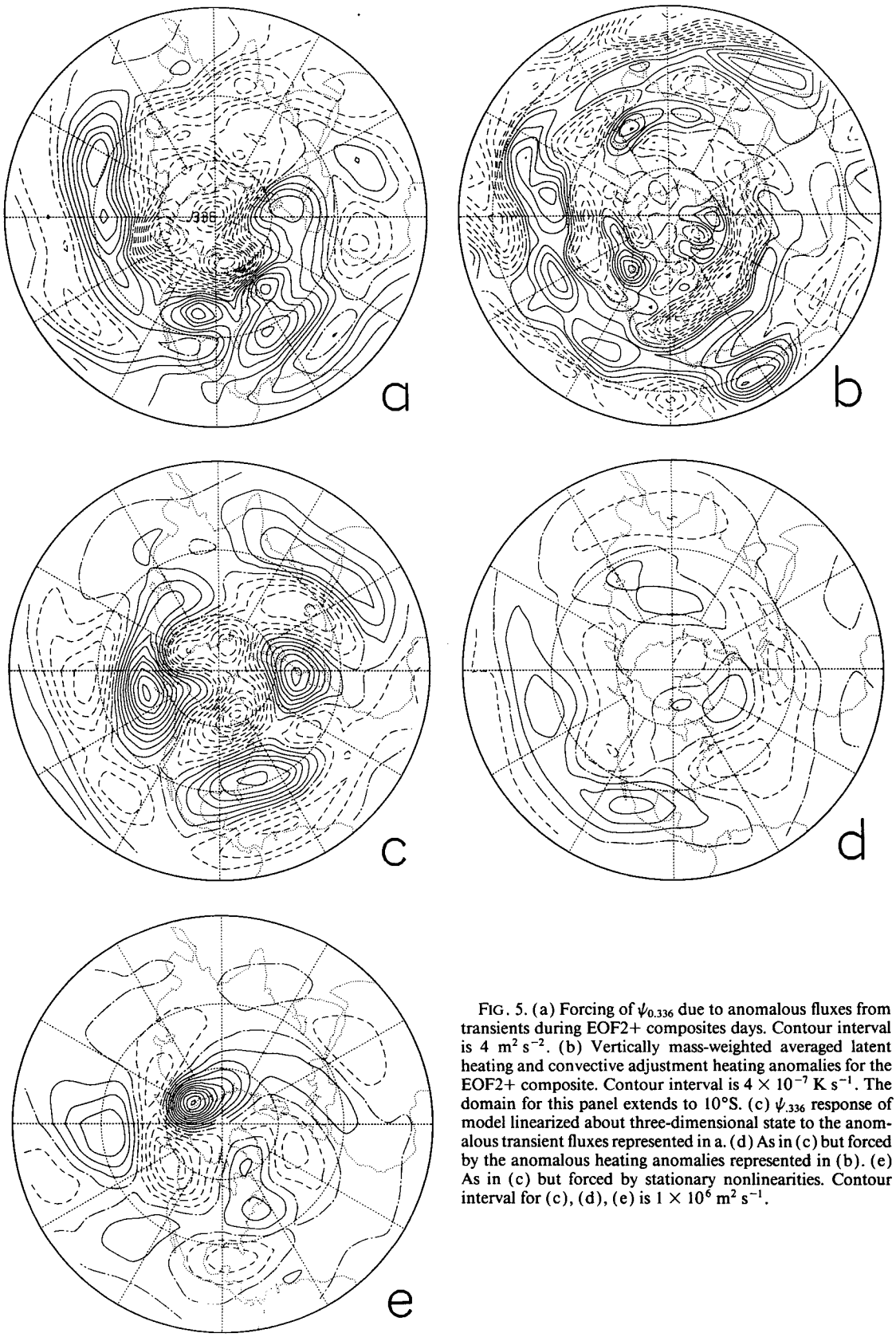

FIG. 5. (a) Forcing of $\psi_{0.336}$ due to anomalous fluxes from transients during EOF2+ composites days. Contour interval is 4 $m^2 s^{-2}$. (b) Vertically mass-weighted averaged latent heating and convective adjustment heating anomalies for the EOF2+ composite. Contour interval is 4×10^{-7} K s^{-1}. The domain for this panel extends to 10°S. (c) $\psi_{.336}$ response of model linearized about three-dimensional state to the anomalous transient fluxes represented in a. (d) As in (c) but forced by the anomalous heating anomalies represented in (b). (e) As in (c) but forced by stationary nonlinearities. Contour interval for (c), (d), (e) is 1×10^6 $m^2 s^{-1}$.

analysis, there is some similarity between the structure of the tendencies generated by the anomalous transients and the structure of the coincident low-frequency anomaly. However, it is only by considering the dynamical effect of these tendencies, as found from the linear model, that one can see how they are transformed into the observed flow anomalies.

The linear response to latent heat and convective adjustment anomalies during EOF2+ episodes is depicted in Fig. 5d. Both from the standpoint of amplitude and of structure, heating anomalies act to make minor modifications to the composite pattern, but no feature appears to be primarily due to this forcing. This is not to say that heating is not strongly associated with the EOF2+ pattern. In Fig. 5b is displayed the vertically averaged latent heating for the EOF2+ composite. Correlation analysis (not shown) indicates that the midlatitude, high-amplitude features on this plot are strongly correlated with occurrences of EOF2, while tropical features are only weakly correlated. For the most part, in midlatitudes these features are consistent with changes in rainfall that one would expect from a synoptic standpoint to result from shifts in storm tracks induced by the presence of the EOF2+ anomalies. Thus, latent heating seems to play an ancillary role in the maintenance of this low-frequency circulation.

The influence of stationary nonlinearities on EOF2+ is to shift the pattern to the west. As seen in Fig. 5e, the response to this term tends to be nearly in quadrature with the response to anomalous transients (Fig. 5c).

Examination of a similar series of plots (not shown) for the EOF2− composite shows that it is maintained in a fashion that is very similar to the way EOF2+ is maintained. Transients are the most important factor. They produce tendencies with nearly the same structure, but opposite sign, as those produced by transients during EOF2+ episodes. Thus, the response to these transients is similar to the response to the anomalous transients found for EOF2+ with signs changed, and produces most of the features in the composite pattern. Latent heating anomalies are also structurally similar to those for EOF2+, with reversed signs, and excite a weak response. The response to stationary nonlinearities is rather substantial in this case, in agreement with the amplitudes plotted in Fig. 4, and is similar not only in structure but in sign to that calculated for EOF2+ (Fig. 5e). This means that nonlinearity has a marked influence on the position of the circulation features in this composite, shifting many of them to the east.

Turning to EOF3, we find that again the main features of the streamfunction composite appear to be maintained by anomalous transient activity. The linear response to anomalous transient fluxes, as displayed in Fig. 6c, produces the four lobes of the pattern (Fig. 1b) in nearly the same positions they are found in the CCM. The structure of the forcing resulting from these transients (Fig. 6a) bears some resemblance to the pattern it forces, but without the help of the linear model it would be difficult to ascertain to what degree it is able to maintain EOF3.

As with EOF2, anomalous latent heating and convective adjustment do not make a strong contribution in midlatitudes, but in the tropics and subtropics the linear budget suggests its effect may be more important. The response to this heating, shown in Fig. 6d, tends to cancel features maintained by transients in the tropical east Pacific, thus emphasizing the midlatitude character of EOF3+. The plot of vertically averaged diabatic heating on EOF3+ days (Fig. 6b) shows large amplitude anomalies in the tropical Pacific that are probably responsible for this part of the response to latent heating. However, correlation analysis indicates that this part of the heating field is not strongly connected with EOF3, and so is likely just a sampling artifact. In contrast to this, central points of the midlatitude feature of Fig. 6b have correlations of about 0.7 with projections of streamfunction onto EOF3. These midlatitude heating anomalies are consistent with shifts in rainfall that one would expect to result from the anomalous troughs and ridges of EOF3+, namely enhanced rainfall on the eastern sides of troughs, suppressed rainfall on the eastern sides of ridges. So, as with EOF2, heating anomalies appear to be subservient features of this pattern.

The effect of stationary nonlinearities on the maintenance of EOF3+ is fairly weak. The linear response to this term is plotted in Fig. 6e and shows that nonlinearity tends to dampen the western lobes of the pattern and shift the eastern lobes eastward.

Plots of the linear response to the various forcing terms that maintain EOF3− primarily serve to reinforce the results of our analysis of the other three low-frequency patterns: Transients are the most important means of maintenance and the influence of heating is weak, except perhaps in the tropics where its significance is questionable. The one way in which the EOF3− budget is fundamentally different is the role it assigns to stationary nonlinearities. From the response to these nonlinearities shown in Fig. 7, we see they make a distinct, positive contribution to the EOF3− composite. Thus, to a certain degree, this pattern is self-sustaining.

6. Further analysis

a. Transients

Having determined that anomalous transients fluxes, in conjunction with the effect of the time-mean flow, are the primary means by which the four patterns we are considering are maintained, we next use the linear budget technique to learn more about the nature of the transients involved in this process. This is done by decomposing the anomalous transient eddy fluxes of each composite into various components of interest, and examining the linear response to each component.

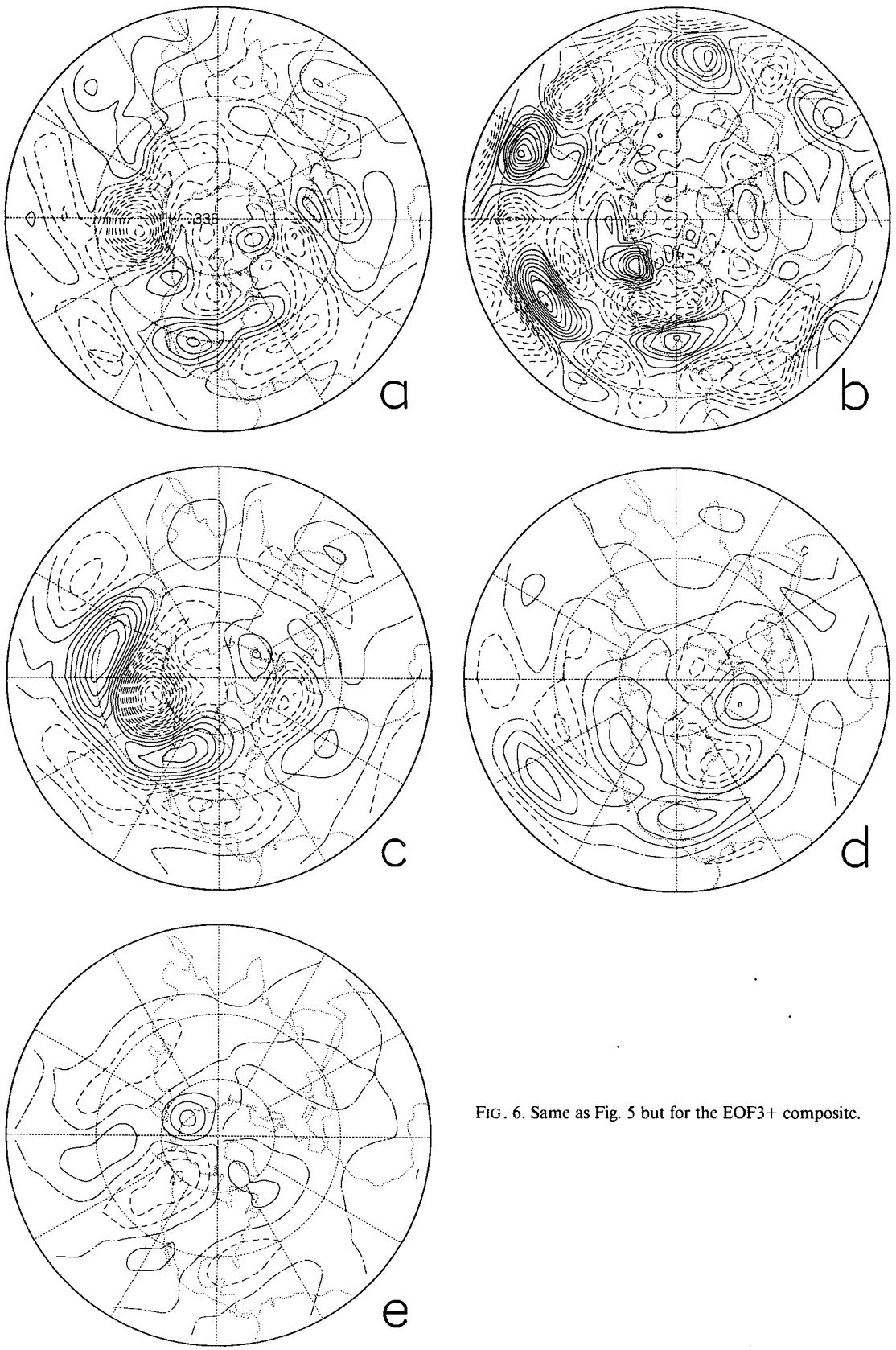

FIG. 6. Same as Fig. 5 but for the EOF3+ composite.

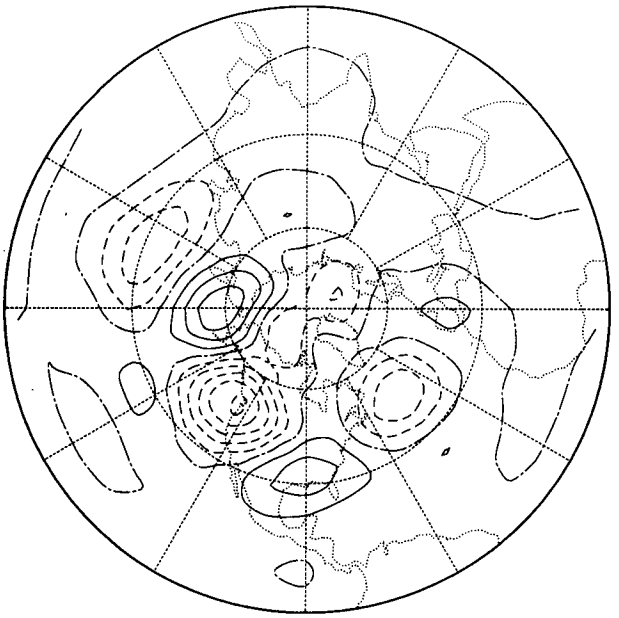

FIG. 7. Response of model linearized about three-dimensional state to stationary nonlinearities of the EOF3− composite. Contour interval is 1×10^6 m^2 s^{-1}.

Again, we rely on the additive property of the responses to make comparison meaningful.

The importance of various components of the anomalous transients is quantified in Table 1, which contains information about the strengths and structure of the linear response to forcing by these components for each composite. Comparison of rows A and H in "a" of this table shows that, just as we saw in Fig. 4, for all four patterns the linear response to all anomalous transients has nearly as much amplitude as the composite streamfunction anomalies. The strength of the response to transients in the vorticity equation (row B) is similar to this amplitude, while the strength of the response to thermal fluxes (row C) is only about 15% of its value. The response to transients acting on the divergence equation is smaller still and is not included in the table. Furthermore, the pattern correlation entries in Table 1b show that the linear response to transients in the vorticity equation (row B) is about the same as the linear response to all transients (row A) in its degree of similarity to the composite flow. Together these facts assign a minor role to thermal fluxes in maintaining the anomalies of the four composites. This is in sharp contrast to studies like those of Nigam et al. (1986) and Lau and Holopainen (1984), who have found that thermal fluxes cannot be ignored when considering the maintenance of the climatological waves. We do not know whether this difference is because we are examining anomalies to the climatological waves, because we are studying a general circulation model, or because our technique considers the response to anomalous fluxes rather than the fluxes themselves.

Further calculations can narrow our description of the transients that maintain the low-frequency anomalies. As substantiated by similarities in the entries of rows B and D in Table 1, the highest-frequency contributions to the transients in the vorticity equation (those not sampled with 12-hourly data) make almost no contribution to the maintenance. This means a residual calculation need not be used to calculate the transients, thus allowing a further refining of our look at transients. For example, if one forces the vorticity equation with only those terms that can be calculated from the rotational component of the wind, the strength and the structure of the response changes little (row E of Table 1). Further narrowing of the time scales of the transients involved can be attained by redefining "transient." To this point in the study, a transient for a pattern composite is a perturbation from the 600-day average that defines the composite. Each composite consists of approximately 25 separate episodes, each consisting of approximately 20 consecutive days, and this definition of transient includes episode-to-episode variability. By redefining transient to mean departures from individual episodes, this very low-frequency variability is removed but, as row F of Table

TABLE 1a. Spatial standard deviation of ψ_{336} in the response of the model linearized about the three-dimensional state to various components of the forcing by anomalous fluxes from transients. A: all forcing by transients, B: vorticity forcing by transients, C: thermal forcing by transients, D: vorticity forcing by transients with periods greater than one day, E: vorticity forcing by rotational transients with periods greater than one day, F: same as E except episode-to-episode variability is ignored, G: vorticity forcing by 1–7-day rotational transients, H: standard deviation of ψ_{336} for the composite. Unit is 10^6 m^2 s^{-1}.

	EOF2+	EOF2−	EOF3+	EOF3−
A	2.2	2.7	1.8	1.8
B	2.2	2.5	1.6	1.5
C	0.3	0.3	0.2	0.3
D	2.2	2.3	1.5	1.1
E	2.3	2.3	1.7	1.2
F	1.9	2.5	1.7	1.4
G	2.2	2.8	1.4	0.8
H	2.6	3.2	1.9	2.3

TABLE 1b. Same as Table 1a except entries are of the spatial correlation between EOF composites and linear responses of ψ_{336}. Only the domain south of 60°N is considered.

	EOF2+	EOF2−	EOF3+	EOF3−
A	.41	.45	.84	.62
B	.45	.66	.76	.45
D	.44	.65	.79	.20
E	.50	.73	.82	.52
F	.61	.71	.85	.48
G	.54	.55	.85	.48

1 indicates, such an effective filtering of the low frequencies has little impact on the influence of the rotational transients.

By bandpass filtering the streamfunction field and using it to calculate the anomalous vorticity forcing during EOF episodes, we can further clarify the time scales of the transients that support the low-frequency structures. We use a 1–7-day Fourier filter to capture variability typically associated with synoptic activity. As depicted in Fig. 8a, this filtering simplifies the vorticity forcing by anomalous fluxes during EOF2+ cases compared with the full vorticity forcing by anomalous transients seen in Fig. 5a. But the response to the filtered transients, shown in Fig. 8c and measured in row G of Table 1, makes a considerable contribution to maintaining EOF2+. Similarly, vorticity forcing of EOF3+ by bandpass vorticity transients (Fig. 8b) is much less complex than the full transient forcing of this pattern

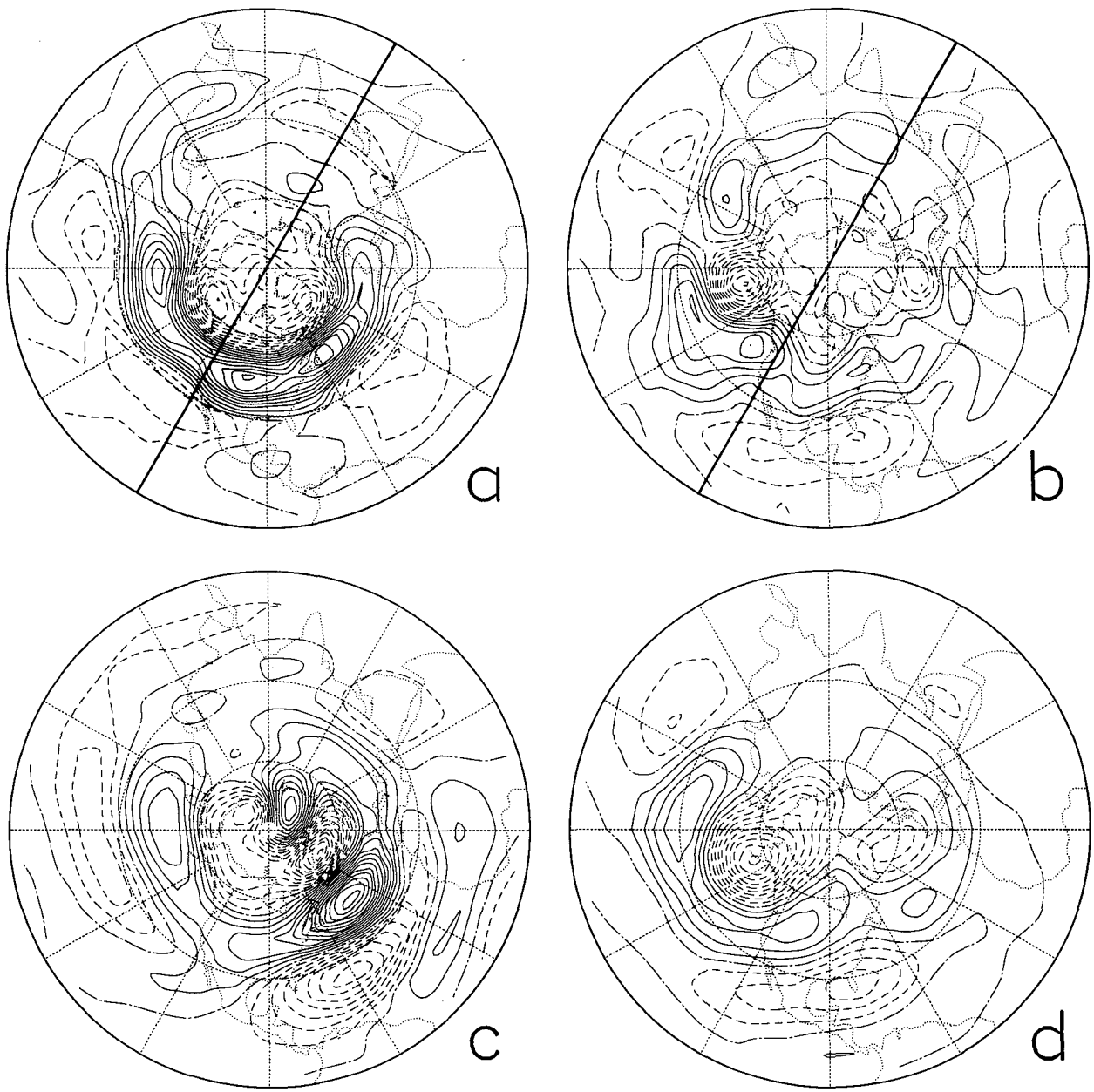

FIG. 8. (a) Forcing of $\psi_{0.336}$ due to anomalous fluxes from nondivergent, 1–7-day bandpass transients for the EOF2+ composite. Contour interval is 2.5 $m^2 s^{-2}$. (b) Same as (a) but for EOF3+. (c) Response of model linearized about three-dimensional state to the forcing represented in (a). Contour interval is 1×10^6 $m^2 s^{-1}$. (d) Same as (c) but for the forcing of (b). [The solid line in (a), (b) shows how the domain is divided for the regional forcing experiments of Fig. 9.]

(Fig. 6a), but its effect (Fig. 8d) is very similar to the effect of all transients (Fig. 6c). The situation, as summarized in Table 1, is much the same for EOF2− and EOF3−. Structurally the forcing and response are essentially the same as for the corresponding two positive EOF composites we have just examined, except the signs of the patterns are different.

Though these results highlight the importance of the bandpass eddies in maintaining the low-frequency composites, they do not indicate that the lower-frequency transients play no maintenance role. Comparison of the structure of the response to all anomalous transients (Fig. 5c) with the response to anomalous fluxes by bandpass transients for EOF2+ shows how the lower-frequency transients can modify the structure of the response. Comparison of the amplitude of the response to bandpass eddies for EOF3− (row G of Table 1a) to that for unfiltered eddies (row E) indicates that in some cases they also have a significant effect on the strength of a pattern.

Another means of distinguishing those transients that most affect the low-frequency composites is by their altitude. If we force the model by the vorticity tendencies caused by anomalous transients at individual levels, we can determine at which level the transients are most important. Whether the influence of transients is measured by the strength of the model's streamfunction response at $\sigma = 0.336$ or $\sigma = 0.664$, composite transient forcing at levels 0.500, 0.336, and 0.189 makes the largest impact. And with the exception of EOF2+, the influence of forcing by transients at 0.336 is always about twice as strong as the influence of forcing at any other level.

As a final step in determining which component of the forcing by anomalous transients is most important in maintaining the EOF composites, we consider the geographical distribution of the transients. Because of the dispersive nature of planetary waves, local sources could be enough to force an entire pattern, and large parts of the forcing distributions we have seen may not be necessary for maintaining the observed anomalies. In fact, a large part of the apparent forcing might, instead, be a result of the flow anomalies. As a crude means of determining whether the nearly hemispheric distributions of diagnosed forcing are actually needed to maintain the EOF composites, we have divided the globe in half at 120°W and 60°E and used the bandpass anomalous vorticity fluxes in the Northern Hemisphere from these halves to force the linear model. This division was chosen because it approximately bisects both EOF2 and EOF3. Figures 9a and 9b show the response for the EOF2+ composite to the forcing from these two sectors. Apparently, forcing from both sectors significantly contributes to EOF2. In each case, the response is primarily in, but not confined to, the hemisphere of excitation. A similar result holds for EOF2−. For EOF3+ the situation is rather different. There, only forcing west of 120°W makes a significant contribution (Fig. 9c). EOF3− also relies only on transients in the western sector to maintain it. So we conclude that eddies from both primary storm tracks of the Northern Hemisphere are acting in concert to maintain EOF2 while only eddies in the Pacific are needed to force EOF3.

b. Stationary nonlinearity

The relatively weak response of the linear operators to the stationary nonlinear terms indicates that, for anomalies with the amplitude of our composites, self-interaction is not a crucial maintenance mechanism. However, the structure of the response to this nonlinearity for the EOF3 composites suggests that for this pattern it may act to skew the distribution of amplitudes of the anomalous flow. Recall that for EOF3+, stationary nonlinearity tended to dampen the strength of the western half of the streamfunction anomaly, while for EOF3− it amplified the entire pattern. This effect should be highly dependent on the amplitude of the low-frequency anomalies since the stationary nonlinear terms are quadratic functions of the anomalies. One might thus expect the action of this term to lead to a cutoff in the potential strength of positive projections onto EOF3, and to encourage large negative projections. Projecting nonoverlapping monthly mean $\psi_{0.336}$ anomalies onto EOF3, we find this very behavior. As depicted in Fig. 10, positive projections of larger than 7 units never occur, while negative projections of as much as 12 units are observed. This leads to a skewness coefficient in the distribution of projection coefficients of −0.39, a level that Monte Carlo tests indicate should only happen by chance about one percent of the time in a sample of 200 like ours. So, for EOF3, stationary nonlinearity is probably influencing the high-amplitude episodes. This is consistent with the White (1980) and Nakamura and Wallace (1991) finding of positive skewness in wintertime upper-tropospheric North Pacific geopotential perturbations and in the Simmons (1982) finding that, in a nonlinear barotropic model, forced anticyclones in the North Pacific tended to be stronger than equally forced cyclones.

c. Zonal-mean perturbations

As discussed in section 4, there is flexibility in the way one subdivides the forcing terms in the linear budget technique. The manner in which we did this subdivision for our budget has prevented us from addressing one maintenance mechanism proposed by Branstator (1984). His work suggested that, to a certain degree, quasi-stationary anomalies in the zonally asymmetric component of atmospheric flow occur as adjustments to changes in the zonal-mean component. Kang (1990) and Nigam and Lindzen (1989) have also considered this mechanism. Because EOF2 has such a strong zonally symmetric component, one might

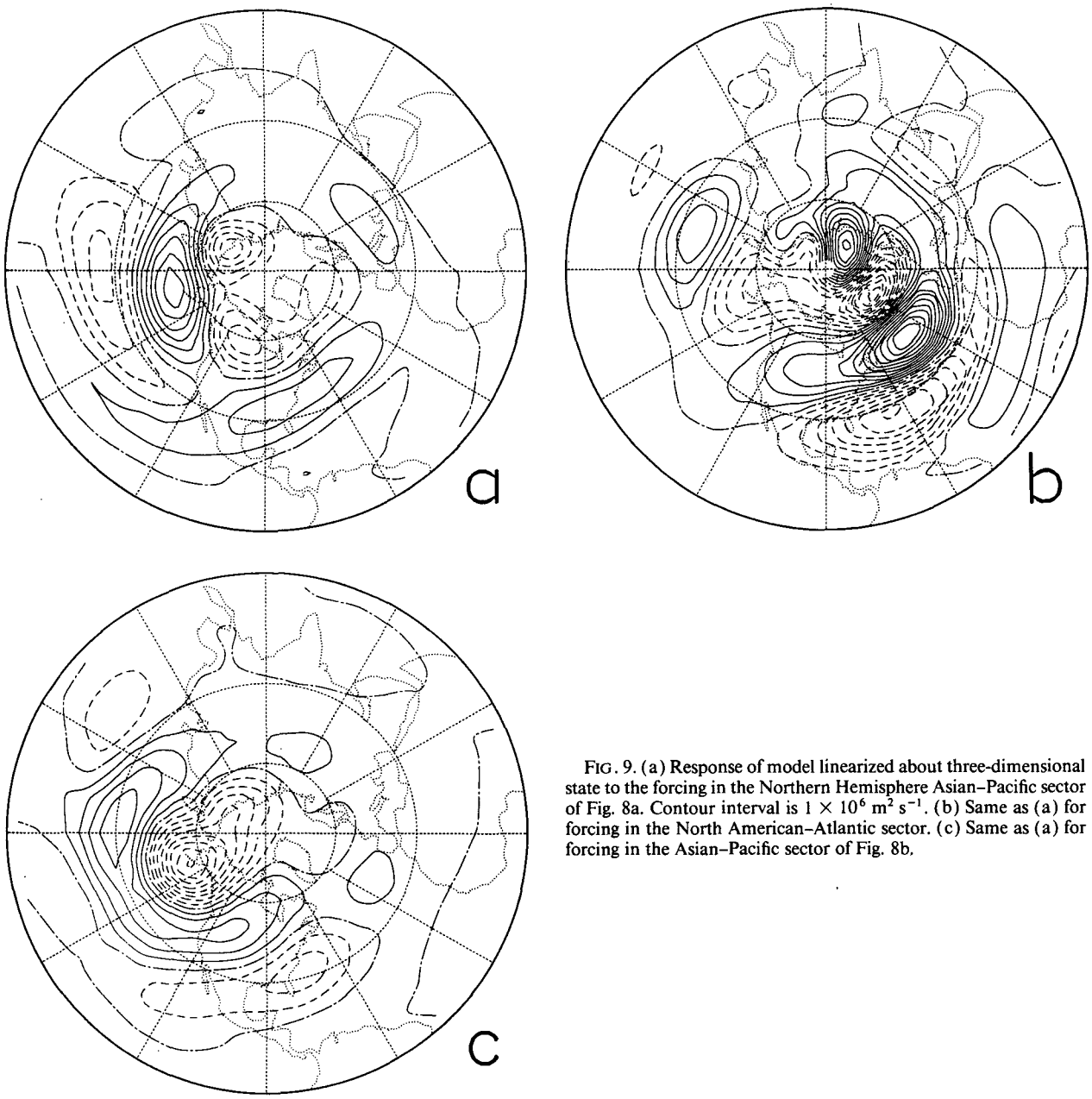

FIG. 9. (a) Response of model linearized about three-dimensional state to the forcing in the Northern Hemisphere Asian–Pacific sector of Fig. 8a. Contour interval is 1×10^6 m^2 s^{-1}. (b) Same as (a) for forcing in the North American–Atlantic sector. (c) Same as (a) for forcing in the Asian–Pacific sector of Fig. 8b.

expect this mechanism to be important in explaining the maintenance of that pattern.

In Branstator (1984) the adjustment of the quasi-stationary waves to anomalies in the time-mean zonal-mean state was defined as the difference between two steady solutions to the nondivergent barotropic vorticity equation linearized about a zonally symmetric state. For one solution the model was linearized about climatological conditions and forced by that function that gave a response exactly equal to the observed climatological waves. For the other solution the same forcing was used, but a zonal-mean anomaly was added to the basic state. To determine how the adjustment of the quasi-stationary waves to zonal anomalies is affecting our composite patterns, we could take this same approach with our baroclinic model and use the zonal mean of the 6000-day climate as one of the basic states in the method and the zonal mean from one of our composites as the other. However, it is useful to notice that if one takes the difference of the model equations for these two cases, the quasi-stationary wave adjustment [defined in the same way and denoted $\Delta(\ )$] can also be found as the steady response of our model linearized about the zonal-mean climate and forced by

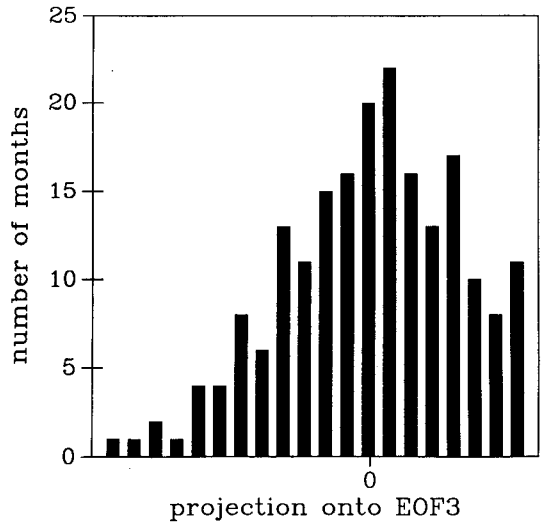

FIG. 10. Number of months for which the projection of EOF3 has a given value. The projection scale is linear.

terms that are functions of the composite anomalies. For example, taking the difference of the thermodynamic energy equation for the two cases gives

$$[\bar{u}^c]\Delta T_x + \cdots = -[\hat{u}]\bar{T}^c_{*x} - [\hat{u}]\hat{T}_{*x} + \cdots \quad (4)$$

where, for simplicity, we have again written down only the horizontal advection terms. Thus, just like the other processes we have considered, the adjustment of the waves to the zonal-mean anomaly can be found as the response to forcing anomalies. In fact, the forcing terms in (4), which represent the interaction of the zonal-mean time-mean anomaly with climate and perturbation waves, were present in our budget of section 4. The first forcing term in (4) was part of the interaction term [C of (3)], and the second forcing term was part of the stationary nonlinearity [A of (3)]. So the adjustment of the waves to zonal-mean anomalies was included in the response we found to these mechanisms. Now, by considering the response to terms like those on the right-hand side of (4), we can see the effect of this process in isolation.

For the EOF2+ composite, when our zonally symmetric operator is forced by all the terms [like those on the right-hand side of (4)] representing interactions with time-mean perturbations of the zonal mean, the response is the flow depicted in Fig. 11. The similarity of this pattern over the Pacific and North America to the zonally asymmetric component of EOF2 (Fig. 1c) is evident. Repeating this calculation with the EOF2− composite (not shown), we find these terms make a similar, in fact stronger, impact on that anomaly. In contrast, these terms seem to have a negligible effect on the EOF3 composites, probably because the zonally symmetric components of those patterns is very weak.

One class of terms involving the zonal-mean component of time-mean perturbations is implicit in the wavy basic-state operator, namely, the class containing terms like $[\hat{u}]\bar{T}^c_{*x}$ that represent the interaction of the time-mean perturbations with the climatological waves. Assuming we can ignore cubic terms, this is probably the dominant class. This follows from the fact that for the anomalous flows we are considering, the time-average perturbations are, in general, weaker than the climatological waves, so, for example, $[\hat{u}]\hat{T}_{*x} < [\hat{u}]\bar{T}^c_{*x}$. Thus, most of the interaction that leads to the perturbations in Fig. 11 should be included implicitly in the budgets of section 5, which used the asymmetric basic-state operator. This interaction contributes more or less to the response to each of the forcing functions considered in that section, depending on whether that function excites a strong or weak zonal-mean anomaly. However, comparison of the zonal-mean components of the EOF2 composite in Fig. 1a to the symmetric part of the response to the sum of all forcing in Fig. A2a indicates that for EOF2 the zonal-mean perturbations tend to be weak in the linear budget with the asymmetric basic-state operator. (This weakness, like all discrepancies between the composites and the linear response to the summed forcing, must ultimately be attributed to the simplified anomalous dissipation of the linear model.) The weak zonal-mean perturbations indicate that, though the adjustment of zonal asymmetries to zonal-mean perturbations can be represented in our linear budget, in fact it is underrepresented. As Fig. 11 showed, this adjustment makes a positive contribution to the main asymmetric features of EOF2, so this underrepresentation should weaken

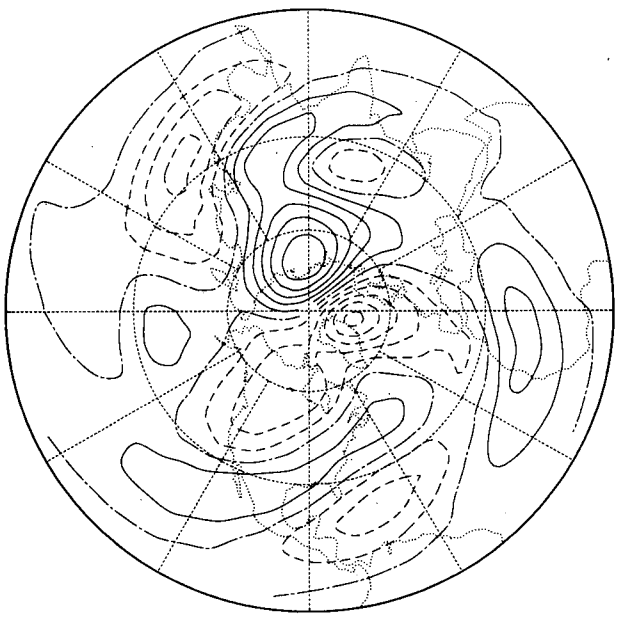

FIG. 11. Response of the model linearized about a two-dimensional state to forcing resulting from perturbations in the time-mean zonal-mean flow for the EOF2+ composite. Contour interval is 1×10^6 $m^2 s^{-1}$.

those features. And, in fact, the linear emulation of EOF2 in Fig. A2a is too weak.

7. Caveats

In section 3 and the Appendix we pointed out that the linear budget technique has drawbacks that result from near resonances in the linear operator and that this problem is especially pronounced for an operator based on a background flow with zonal asymmetries. However, given the evidence that interactions with these asymmetries are essential to the dynamics that influences low-frequency anomalies, we have chosen to include these interactions and control the resonances with appropriate dissipation.

There are other properties of the approach we have taken that should be kept in mind when interpreting our findings. The way that the forcing was separated into various terms in (2) and (3) is not unique and perhaps not even the best possible separation. In particular, the distinction between stationary nonlinearities (term A) and transients (term B) is problematic in that nonlinearities involving low-frequency departures from the climatological mean are included in both terms A and B. For this reason, the bandpass transients considered in section 6 are probably a more physically meaningful flow component than the transients of earlier sections.

In order to focus on robust aspects of the maintenance of low-frequency patterns, composites have been used. This leads to the possibility that very different situations may be intertwined in the analyzed structures. For example, EOF3− appears to be maintained by both anomalous transient fluxes and stationary nonlinearities. This does not necessarily mean that in all episodes that contributed to the EOF3− composite both mechanisms were important. In fact, one would expect that, for the lower-amplitude episodes, stationary nonlinearity would be relatively less important. It may even be that for isolated cases, sources (like latent heating) that seem unimportant for the composite could be all-important.

It should also be remembered that the analysis was for four particular patterns and the conclusions may not be relevant for other low-frequency structures occurring in the CCM simulation. In fact, strictly speaking, the results cannot be applied to linear combinations of these four patterns. However, one can show that if transients and stationary nonlinearities are combined into a single nonlinear forcing term, then the effects of nonlinearity are additive, as are the effects of the diabatic term. Thus, the impact of heating anomalies on maintaining a composite that consists of the sum of two of our patterns is the sum of the impact of heating on the individual patterns, and similarly for nonlinear forcing. Hence, to the degree that transients are dominant over stationary nonlinearity, one can then predict that, for combinations of the patterns, anomalous transients will be the primary maintenance mechanism.

Furthermore, that we have examined composites consisting of days when a given pattern was strong, but not necessarily growing, means that our study is in fact one of maintenance and not of causality or initiation. Other mechanisms than the ones we have isolated may be important during those periods when a pattern is amplifying.

The question of causality may have a very different answer than the question of maintenance. One can imagine the possibility that the anomalous transient fluxes we found so important are actually the result of an adjustment to heating anomalies, which could then be viewed as the instigators of the low-frequency anomalies. Indeed, in analyzing a GCM simulation of the response to El Niño heating, Held et al. (1989) found that transients apparently induced by the heating anomaly were the main means by which the flow anomaly in their experiment was maintained.

Finally, as in all such studies, one cannot be certain that the general circulation model experiment we have examined is a good analog to nature. That its low-frequency patterns are similar to those in nature makes it a simulation worth studying, but known simplifications of the model (e.g., constant sea surface temperatures and no annual cycle) could be coloring our results.

8. Conclusions and discussion

Even with the uncertainties inherent in the approach we have taken, there can be little doubt that there are two main mechanisms at work in the maintenance of the leading midlatitude low-frequency anomalies in the simulation studied here. One mechanism is the dynamical interaction between the anomalies and the time-mean flow and the other is the influence of anomalous transient eddy fluxes. The former can be divided into the effects of the zonal-mean time-mean flow with its well-known impact on the dispersion of large-scale anomalies (cf. Hoskins and Karoly 1981) and the effects of the time-mean eddies, which modify the dispersion process (cf. Branstator 1983) and act as an internal energy source (cf. Simmons et al. 1983; Branstator 1990). Based on the linear budget with a zonally symmetric basic state, this internal source accounts for roughly half the amplitude of our composite anomalies. The remaining amplitude appears to be maintained by specially configured anomalous transients. Our analysis indicates that this maintenance is primarily affected by the momentum fluxes associated with these transients and that upper-tropospheric transients with time scales less than seven days account for much, but not all, of the maintenance.

Two secondary processes also appear to be involved in the workings of the low-frequency anomalies. Nonlinear interactions of the time-averaged perturbations

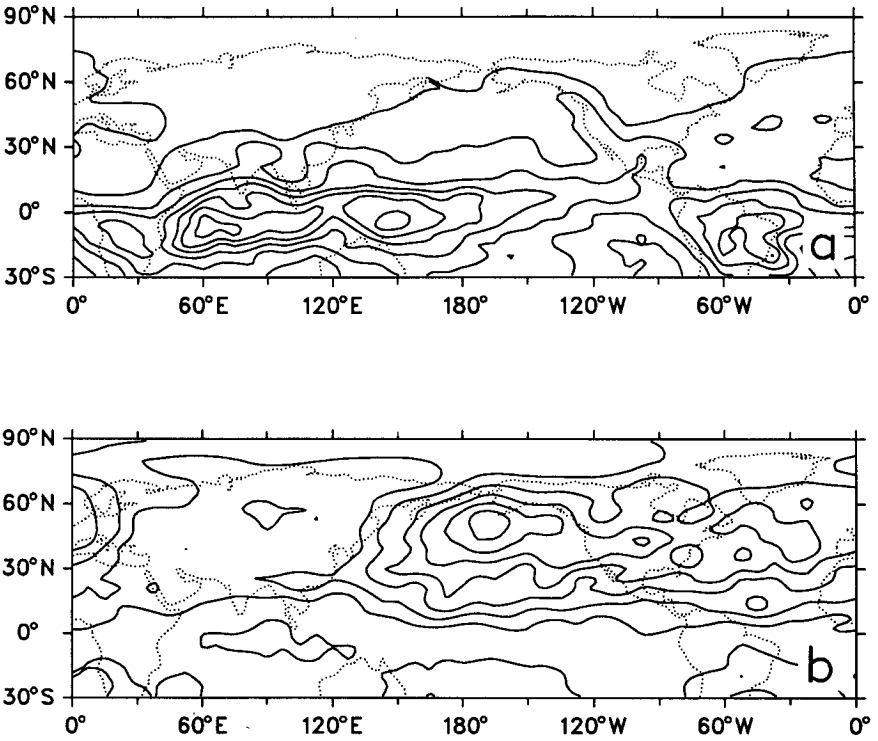

FIG. 12. (a) Standard deviation of monthly mean daily rainfall rate during a perpetual January GCM experiment. Contour interval is 0.6 mm/day. (b) Standard deviation of monthly means of $\psi_{0.336}$ forcing due to nondivergent transients (i.e., the standard deviation of $-\nabla^{-2}\overline{\nabla\zeta'_\psi \cdot \nabla\zeta'}$, where bar is a monthly average and prime is deviation from that average). Contours range from 12 to 33 $m^2\ s^{-2}$ with an interval of 3 $m^2\ s^{-2}$.

with themselves, especially in the case of EOF3, act to dampen one polarity of the pattern and strengthen the other, leading to a skewed distribution of amplitudes. These same interactions cause phase shifts in the features of EOF2. Interactions between the zonal-mean and zonally asymmetric components of EOF2 help to maintain this pattern, which has a pronounced zonal-mean component.

Of the potential low-frequency maintenance mechanisms outlined in the Introduction, diabatic heating anomalies appear to have the smallest impact in our CCM simulation. One might wonder if this conclusion is strongly influenced by the fact that the simulation has fixed sea surface temperature and thus, perhaps, weak low-frequency heating fluctuations. Estimates of rainfall variability in nature have been made by Taylor (1973), Shukla (1988), and Shea (1986) from island, satellite, and combined observing systems, respectively. Comparison of their results with rainfall variability in the CCM (Fig. 12a) suggests four regions where the CCM's variability could be weak. In the equatorial zone just east of the date line CCM variance is almost certainly too weak, probably because El Niño events are not felt by the model. Extratropical North Pacific variability also seems rather weak. The CCM does have maxima of variability over Indonesia and the Amazon, which have magnitudes similar to observational estimates, but given the uncertainty of the observations, the large values of variability in these regions are also potentially underestimated.

Information about the possible consequences of weak rainfall anomalies in our simulation can be gleaned from the linear model. It can be used to estimate those locations at which the direct effect of heating anomalies is most effective at stimulating our low-frequency patterns. Imposing a steady heating in the model that is zero at all but one point and has the form $\sin\pi\sigma$ at that point, where σ is the vertical coordinate, we find the effect of an isolated source. Spatially correlating that response with an EOF indicates the impact of that source on the production of the EOF pattern, and plotting those correlations at the location of the source provides a chart of the contribution that heating at each location on the globe makes to the EOF structure.[2] When this procedure is applied to EOF2, the plot in Fig. 13a is produced. This chart indicates that, of the regions identified as potentially having weak

[2] Alternatively, plots of the projection of each response onto the EOF can be made. In our application, plots of projections are structurally similar to plots of correlations.

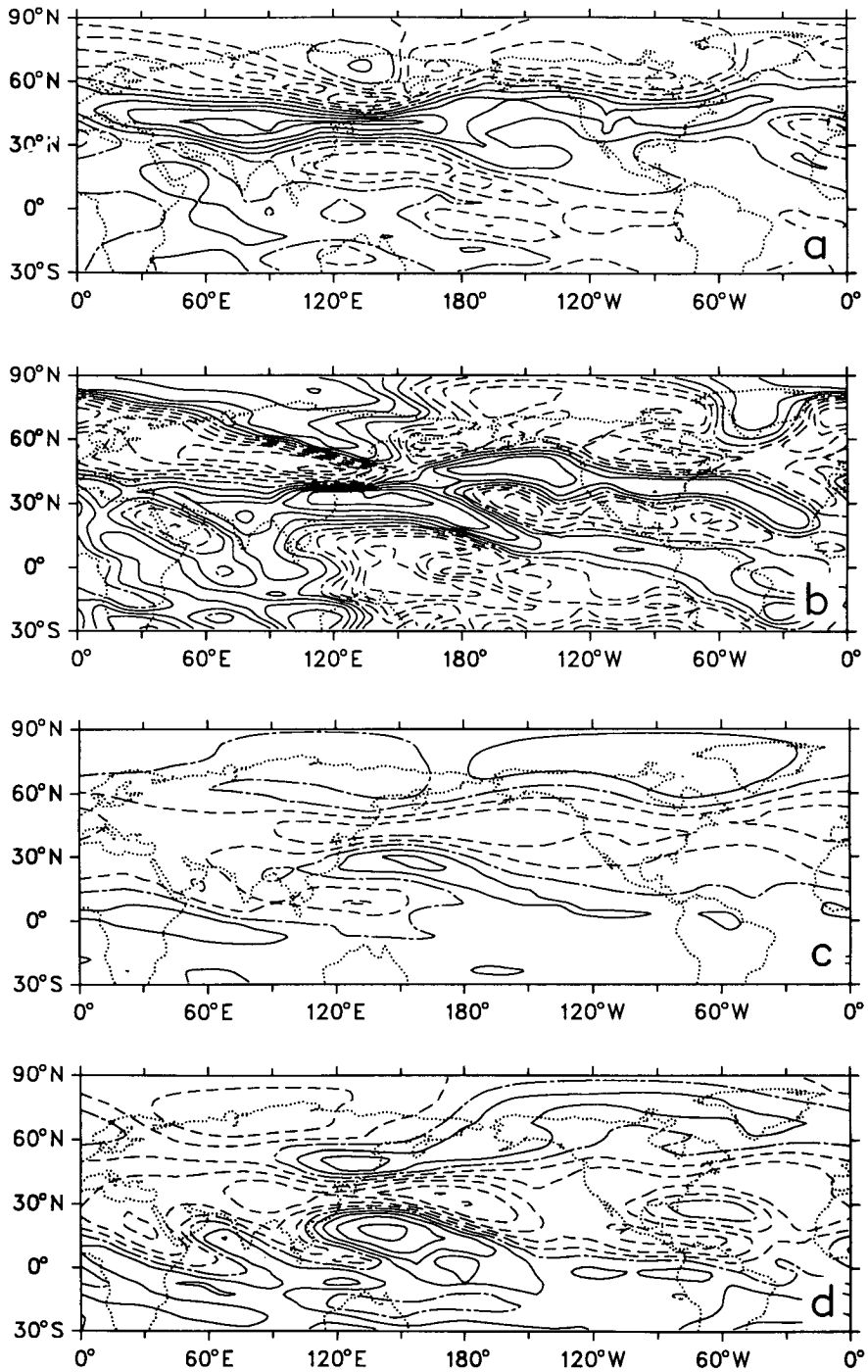

FIG. 13. Correlation between an EOF and the response of a model linearized about a three-dimensional state to forcing at the point where the correlation is plotted. (a) Thermal forcing of EOF2, (b) thermal forcing of EOF3, (c) vorticity forcing of EOF2, (d) vorticity forcing of EOF3. Contour interval is 0.15.

diabatic heating anomalies in the CCM, only the equatorial central Pacific and extratropical North Pacific could make a significant contribution to the maintenance of EOF2. The possibility of western Pacific heating anomalies helping to maintain EOF2 is in accord with the Pitcher et al. (1988) experiments, which showed that an essentially identical version of the CCM responded to a cold pool in the western North Pacific

Ocean by producing a flow anomaly very similar to negative episodes of our EOF2.

The corresponding plot in Fig. 13b for EOF3 shows more potential for contributions from heating that could be produced by SST anomalies. From that diagram it appears that enhanced equatorial Pacific rainfall anomalies west of the date line would contribute to the pattern. Furthermore, there are locations in midlatitudes, particularly in the Pacific and eastern Asia, from which heating is more adept at forcing EOF3 than is tropical heating. Using a GCM with time-varying SSTs, Lau and Nath (1990), too, found that certain locations in the midlatitude North Pacific were able to excite an atmospheric anomaly very much like our EOF3.

Though the results of our point heating source calculations indicate that in systems with time-varying bottom boundaries heating anomalies may prove to be relatively more important than our budgets suggest, this fact does not override the basic fact that internally generated low-frequency variations in fluxes by high-frequency transients by themselves can, and probably do, maintain conspicuous low-frequency patterns.

One possible explanation for the prominence of vorticity fluxes in the maintenance of CCM low-frequency anomalies can be discovered by again considering the linear response to point sources. This time we use vorticity forcing that is zero everywhere except at one point where it has the value one at levels $\sigma = 0.189$ and 0.336 and one-half at $\sigma = 0.500$. [This distribution is meant to approximate the vertical distribution of momentum fluxes that Lau (1978) found to be typically associated with midlatitude bandpass transients.] The correlations between the response to these point sources and EOF2 and EOF3, displayed in Figs. 13c and 13d, show a good deal of overlap between the region where CCM low-frequency variability in transient fluxes tends to be largest (Fig. 12b) and the points that are best at forcing the prominent EOFs. This overlap is in contrast to the situation for heating; there the overlap between heating anomalies (Fig. 12a) and efficient excitation sites (Figs. 13a and 13b) is slight. This advantage must contribute to the dominance of transient vorticity fluxes in our budgets.

The point source calculations summarized in Figs. 13c and 13d can also be used to draw conclusions about the structure of transients that help maintain low-frequency anomalies in the CCM simulation. Both Egger and Schilling (1983) and Branstator (1990) have demonstrated that transients with no organized structure (except, in the case of Egger and Schilling, geographical localization) could be responsible for the observed geographical distribution of low-frequency variability. According to this viewpoint, the particular distribution of transients that is required to support a given low-frequency anomaly occasionally occurs by chance. If this were the state of affairs in the CCM, then the distribution of vorticity forcing in our composites (i.e., the Laplacian of Figs. 5a and 6a) would have the same structure as the plots of correlation coefficients in Figs. 13c and 13d. But in fact, when such a comparison is made, we find very little in common between the plots of the vorticity sources that actually maintain the anomalies and the plots showing the most effective means of maintaining the anomalies. From this we conclude that some process must be organizing the high-frequency transients so that the low-frequency vorticity sources they produce are not randomly distributed in space. Moreover, this organization must go beyond the geographical localization seen in Fig. 12b; localization alone would produce forcing patterns like the dot product of Fig. 12b and Figs. 13c and 13d.

We noticed in section 5 that diabatic heating anomalies that accompany EOF episodes may be organized by the low-frequency flow anomalies. This may also be the case for the transient vorticity fluxes. This possibility is in accord with recent findings by Cai and Mak (1990) and Robinson (1991), who have found evidence in simple nonlinear models that low-frequency anomalies may organize high-frequency transients in such a way that they, in turn, help to maintain the low-frequency anomalies. It is also consistent with the two-way interaction between high- and low-frequency anomalies noted by Kushnir and Wallace (1989) in medium-range forecasts.

Low-frequency anomalies like the ones we have considered are thought to be flow components that are potentially predictable beyond the two-week limit offered by predictability theory. Our results have some bearing on this possibility. First, our analysis shows that the low-frequency variability previously documented by Lau (1981) and Chervin (1986) in general circulation model simulations that exclude intraseasonal sea surface temperature variability need not be produced by tropical heating anomalies. Thus, a large fraction of midlatitude low-frequency variability may not be subject to the enhanced predictability associated with variability caused by slowly changing boundary conditions.

Second, the analysis indicates that, just as the experiments of Palmer and Mansfield (1985) and Blackmon et al. (1987) showed that a correct simulation of the stationary climatological waves is crucial for the correct prediction of midlatitude anomalies induced by tropical heating, these waves must be correctly produced for the accurate prediction of anomalies maintained by midlatitude transients.

Third, our results call into question the very notion that low-frequency anomalies may be especially predictable; to a large degree, their maintenance relies on high-frequency anomalies whose predictability is known to be limited. This pessimistic view would be valid if the atmosphere relied solely on linear interactions between the time-mean flow and high-frequency transients for the maintenance of the low-frequency anomalies. However, in this section we have

argued that there is reason to believe the anomalous transient fluxes that maintain the patterns are organized, perhaps by the low-frequency patterns, as Robertson and Metz's (1989) linear calculations suggest is possible. In experiments to be reported elsewhere we have found the changes in the quasi-stationary flow caused by the presence of EOF2 or EOF3 are sufficient to produce the reorganization of the transients observed in the CCM simulation during EOF2 and EOF3 episodes. Thus, it may be that, because the very presence of a low-frequency anomaly can produce the required anomalous transient eddy statistics, the maintenance of long-lasting anomalies beyond two weeks is possible in long-range forecasts. Hence, our basic finding that anomalous transient eddy fluxes and their interaction with the climatological waves are the primary means of maintaining low-frequency anomalies need not preclude the possibility of extended-range forecasts.

Acknowledgments. Some of the ideas expressed in this paper developed in part from discussions with D. Baumhefner, H. Nakamura, and J. Tribbia. The readability of the text benefited from reviews of an earlier version of the exposition by R. Errico and A. Kasahara. R. Bailey prepared the manuscript and A. Mai refined several of the figures. The work was partially funded by the National Oceanic and Atmospheric Administration under P.O. NA88AANG0140 and the National Aeronautics and Space Administration under Project UPN 578-41-31-03.

APPENDIX

Dissipation in the Linear Budget

Except for very small errors, like those resulting from temporal data sampling, the discretized form of (2) and its companion equations is exact. But if one uses that system (in which the Fickian term is the only dissipation) to interpret stationary anomalies as the forced response to the right-hand-side terms, one finds there is large cancellation in the response to separate components of the forcing, and the response is sensitive to small forcing changes. This behavior indicates the existence of nearly resonant modes in the linear system, and eigenanalysis of the operator can confirm this.

At the truncation used for forced solutions throughout this paper the discretized operator on the left-hand side of (2) contains 9408 degrees of freedom, making eigenanalysis impractical. Reducing its order by truncating spectral representation of variables at zonal wavenumber 6 while retaining 16 meridional modes for each wavenumber makes eigenanalysis possible. Judging by the forced behavior of this truncated operator, its characteristics are very similar to those of the higher-resolution operator. The spectrum of the reduced operator, as given by EISPACK routines using elementary similarity transformations and the QR method, is displayed in Fig. A1a. The mass of eigenvalues near the origin confirms that there are many structures that are nearly resonant to steady forcing. In this way the spectrum is similar to those of the barotropic vorticity equation linearized about climatological flows, as reported by Branstator (1985), though the barotropic spectrum has fewer eigenvalues near the origin.

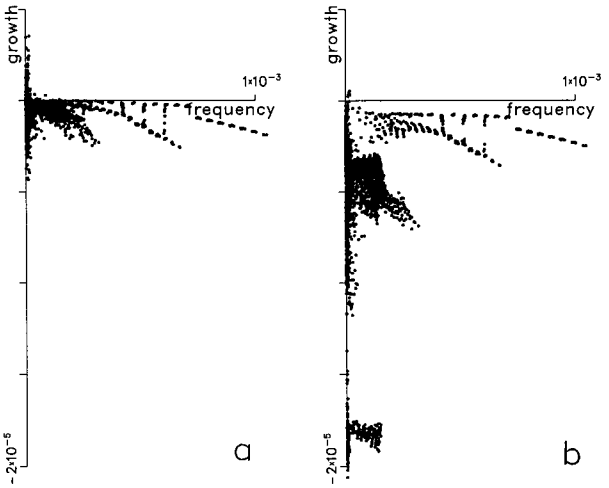

FIG. A1. Eigenspectrum of the baroclinic linear model used in this study, truncated to zonal wave 6, when it has a three-dimensional basic state. (a) The only dissipation included is Fickian horizontal diffusion. (b) The same Fickian, Rayleigh, Newtonian, and vertical diffusion used in our forced experiments is included.

To control these near singularities in the operator we add the dissipation terms mentioned in section 3. With these included, the spectrum is as in Fig. A1b. As one would expect, the dissipation has the general effect of reducing growth rates. There are still many modes with low frequency, but few are close enough to being neutral to be quasi-singular. Thus, the response of this operator is much less sensitive to small modifications in forcing than the weakly dissipated operator of Fig. A1b.

Still stronger dissipation would remove all traces of resonance, but we believe this would have been unphysical. Two pieces of evidence suggest that the employed dissipation is appropriate for our study. 1) It was with this same dissipation that Branstator (1990) found this model (at the zonal wavenumber 6 truncation) had preferred low-frequency patterns whose structure and prominence was similar to low-frequency patterns in the CCM. Reapplication of the procedures used by Branstator (1990) shows that the model has this same property when truncated at zonal wave 10, as in the current study. This suggests that the correct family of modes is allowed to be near resonance by this choice of dissipation. 2) When the viscous linear operator is forced by all the forcing terms except $\hat{D}$ in (2) and the companion equations, as diagnosed to occur in the CCM during episodes of low-frequency EOFs, the linear response is similar to the EOF com-

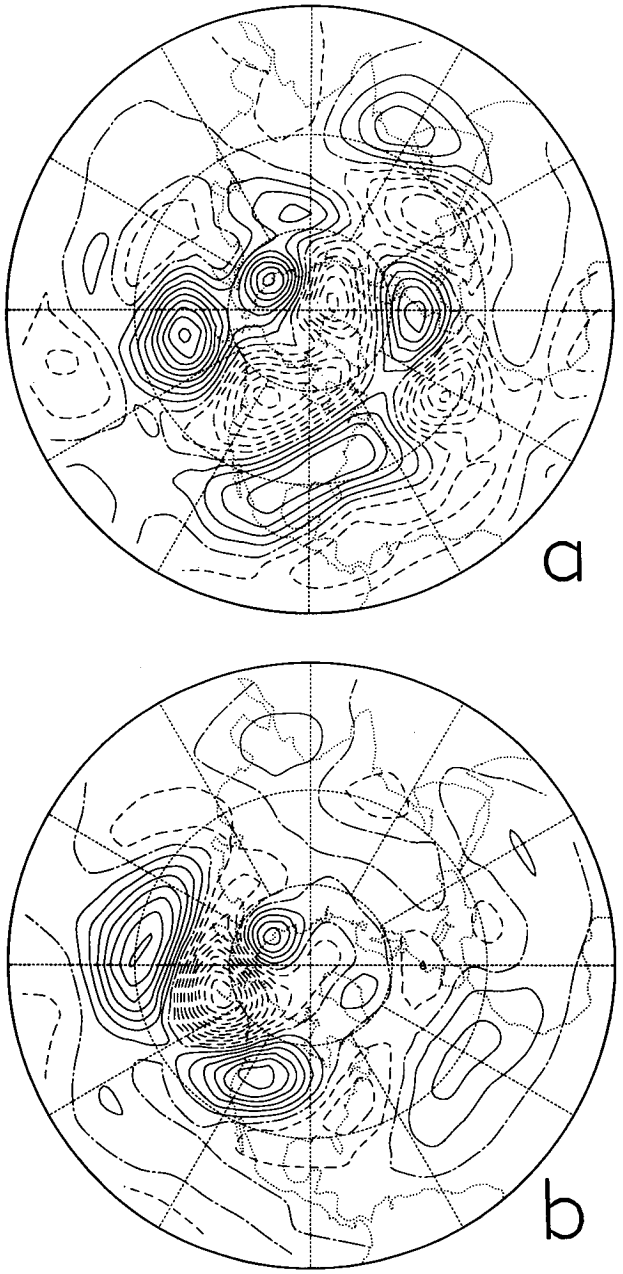

FIG. A2. Response of the model linearized about a three-dimensional state to the sum of all diagnosed forcing terms for composites of (a) EOF2+, (b) EOF3+. Contour interval is 1×10^6 m^2 s^{-1}.

posites. Figures A2a and A2b are examples of such forced solutions. The similarity between these patterns and the composites of Fig. 1 indicates that the linear dissipation is both controlling the resonances of inviscid operators and approximating the perturbation dissipation that actually occurs during episodes of the anomalies we are studying.

Though we believe the particular dissipation employed has its merits, the fact remains that our results are affected by this choice. One way to see this is to consider a scale-independent modification to the dissipation, that is, one of the form $\alpha\xi$ on each of the model's primary fields ξ. Such a modification has the effect of moving each eigenvalue up or down a fixed distance in a plot like Fig. A1. Thus, such a change in the dissipation will bring different eigenmodes closer to or farther from resonance, and hence affect the model's response to a given forcing function.

For the operator based on a zonally symmetric basic state used in section 4, resonance is not as important an issue. Without the basic-state asymmetries, there are no low-frequency modes with significant growth rates, and so no mode is nearly resonant to stationary forcing, provided dissipation of the strength commonly used is employed.

REFERENCES

Blackmon, M. L., G. W. Branstator, and G. T. Bates, 1987: An analysis of equatorial Pacific sea surface temperature anomaly experiments in general circulation models with and without mountains. *J. Atmos. Sci.*, **44**, 1828–1844.

Branstator, G., 1983: Horizontal energy propagation in a barotropic atmosphere with meridional and zonal structure. *J. Atmos. Sci.*, **40**, 1689–1708.

——, 1984: The relationship between zonal mean flow and quasi-stationary waves in the midtroposphere. *J. Atmos. Sci.*, **41**, 2163–2178.

——, 1985: Analysis of general circulation model sea-surface temperature anomaly simulations using a linear model. Part II: Eigenanalysis. *J. Atmos. Sci.*, **42**, 2242–2254.

——, 1990: Low-frequency patterns induced by stationary waves. *J. Atmos. Sci.*, **47**, 629–648.

——, and J. D. Opsteegh, 1989: Free solutions of the barotropic vorticity equation. *J. Atmos. Sci.*, **46**, 1799–1814.

Cai, M., and M. Mak, 1990: Symbiotic relation between planetary and synoptic scale waves. *J. Atmos. Sci.*, **47**, 2953–2968.

Chervin, R. M., 1986: Interannual variability and seasonal climate predictability. *J. Atmos. Sci.*, **43**, 233–251.

Egger, J., and H.-D. Schilling, 1983: On the theory of the long-term variability of the atmosphere. *J. Atmos. Sci.*, **40**, 1073–1085.

Frederiksen, J., 1983: A unified three-dimensional instability theory of the onset of blocking and cyclogenesis. II: Teleconnection patterns. *J. Atmos. Sci.*, **40**, 2593–2609.

Held, I. M., S. W. Lyons, and S. Nigam, 1989: Transients and the extratropical response to El Niño. *J. Atmos. Sci.*, **46**, 163–174.

Horel, J. D., and J. M. Wallace, 1981: Planetary-scale atmospheric phenomena associated with the Southern Oscillation. *Mon. Wea. Rev.*, **109**, 813–829.

Hoskins, B. J., A. J. Simmons, and D. C. Andrews, 1977: Energy dispersion in a barotropic atmosphere. *Quart. J. Roy. Meteor. Soc.*, **103**, 553–567.

——, and D. J. Karoly, 1981: The steady linear response of a spherical atmosphere to thermal and orographic forcing. *J. Atmos. Sci.*, **38**, 1179–1196.

Kang, I.-S., 1990: Influence of zonal mean flow change on stationary wave fluctuations. *J. Atmos. Sci.*, **47**, 141–147.

Kok, C. J., and J. D. Opsteegh, 1985: On the possible causes of anomalies in seasonal mean circulation pattern during the 1982–83 El Niño event. *J. Atmos. Sci.*, **42**, 677–694.

Kushnir, Y., and J. M. Wallace, 1989: Interaction of low- and high-frequency transients in a forecast experiment with a general circulation model. *J. Atmos. Sci.*, **46**, 1411–1418.

Lau, N.-C., 1978: On the three-dimensional structure of the observed transient eddy statistics of the Northern Hemisphere wintertime circulation. *J. Atmos. Sci.*, **35**, 1900–1923.

——, 1981: A diagnostic study of recurrent meteorological anomalies appearing in a 15-year simulation with a GFDL general circulation model. *Mon. Wea. Rev.*, **109,** 2287–2311.

——, 1988: Variability of the observed midlatitude stormtracks in relation to low-frequency changes in the circulation pattern. *J. Atmos. Sci.*, **45,** 2718–2743.

——, and E. O. Holopainen, 1984: Transient eddy forcing of the time-mean flow as identified by quasi-geostrophic tendencies. *J. Atmos. Sci.*, **41,** 313–328.

Metz, W., 1989: Low-frequency anomalies of atmospheric flow and the effects of cyclone-scale eddies: A canonical correlation analysis. *J. Atmos. Sci.*, **46,** 1026–1041.

Nakamura, H., and J. M. Wallace, 1990: Observed changes in baroclinic wave activity during the life cycles of low-frequency circulation anomalies. *J. Atmos. Sci.*, **47,** 1100–1116.

——, and ——, 1991: On the skewness of low-frequency fluctuations in the tropospheric circulation during the Northern Hemisphere winter. *J. Atmos. Sci.*, **48,** 1441–1448.

Nigam, S., and R. S. Lindzen, 1989: The sensitivity of stationary waves to variations in the basic state zonal flow. *J. Atmos. Sci.*, **46,** 1746–1768.

——, I. M. Held, and S. W. Lyons, 1986: Linear simulation of the stationary eddies in a general circulation model. Part I: The no-mountain model. *J. Atmos. Sci.*, **43,** 2944–2961.

Palmer, T. N., and D. A. Mansfield, 1986: A study of wintertime circulation anomalies during past El Niño events, using a high resolution general circulation model. I: Influence of model climatology. *Quart. J. Roy. Meteor. Soc.*, **112,** 613–638.

Pitcher, E. J., M. L. Blackmon, G. T. Bates, and S. Munoz, 1988: The effect of North Pacific sea surface temperature anomalies on the January climate of a general circulation model. *J. Atmos. Sci.*, **45,** 173–188.

Robertson, A. W., and W. Metz, 1989: Three-dimensional linear instability of persistent anomalous large-scale flows. *J. Atmos. Sci.*, **46,** 2783–2801.

Robinson, W. A., 1991: The dynamics of low-frequency variability in a simple model of the global atmosphere. *J. Atmos. Sci.*, **48,** 429–441.

Shea, D. J., 1986: *Climatological Atlas: 1950–1979. Surface Air Temperature, Precipitation, Sea-Level Pressure, and Sea-Surface Temperature (45°S–90°N).* NCAR Tech. Note NCAR/TN-269+STR. Boulder, CO.

Shukla, J., 1988: Variability of rainfall over tropical oceans: Scientific basis and justification for TRMM. *Tropical Rainfall Measurement,* J. S. Theon and N. Fugano, Eds., A. Deepak, 75–79.

Simmons, A. J., 1982: The forcing of stationary wave motion by tropical diabatic heating. *Quart. J. Roy. Meteor. Soc.*, **108,** 503–534.

——, J. M. Wallace, and G. W. Branstator, 1983: Barotropic wave propagation and instability, and atmospheric teleconnection patterns. *J. Atmos. Sci.*, **40,** 1363–1392.

Taylor, R. C., 1973: *An Atlas of Pacific Island Rainfall.* Data Report No. 25, Hawaii Institute of Geophysics, University of Hawaii.

Trenberth, K. E., and G. W. Branstator, 1992: Issues in establishing causes of the 1988 drought over North America. *J. Climate,* **5,** 159–172.

Tribbia, J. J., 1984: Modons in spherical geometry. *Geophys. Atrophys. Fluid Dyn.*, **30,** 131–168.

Valdes, P. J., and B. J. Hoskins, 1989: Linear stationary wave simulations of the time mean climatological flow. *J. Atmos. Sci.*, **46,** 2509–2527.

Verkley, W. T. M., 1984: The construction of barotropic modons on a sphere. *J. Atmos. Sci.*, **41,** 2492–2504.

White, G. H., 1980: Skewness, kurtosis and extreme values of Northern Hemisphere geopotential heights. *Mon. Wea. Rev.*, **108,** 1446–1455.

Williamson, D. L., 1983: Description of the NCAR Community Climate Model (CCM0B). NCAR Tech. Note, NCAR/TN-210+STR, 88 pp.

——, and G. S. Williamson, 1984: Circulations statistics from January and July simulations with the NCAR Community Climate Model (CCM0B). NCAR Tech. Note, NCAR/TN-244+STR.